High-solids anaerobic digestion model for homogenized reactors

Vicente Pastor Poquet, Stefano Papirio, Jean-Philippe Steyer, Eric Trably, Renaud Escudié, Giovanni Esposito

Accepted Manuscript

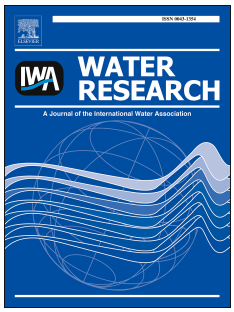

High-solids anaerobic digestion model for homogenized reactors

Vicente Pastor-Poquet, Stefano Papirio, Jean-Philippe Steyer, Eric Trably, Renaud Escudié, Giovanni Esposito

PII: S0043-1354(18)30460-3

DOI: 10.1016/j.watres.2018.06.016

Reference: WR 13843

To appear in: *Water Research*

Received Date: 19 March 2018

Revised Date: 22 May 2018

Accepted Date: 7 June 2018

Please cite this article as: Pastor-Poquet, V., Papirio, S., Steyer, J.-P., Trably, E., Escudié, R., Esposito, G., High-solids anaerobic digestion model for homogenized reactors, *Water Research* (2018), doi: 10.1016/j.watres.2018.06.016.

Graphical Abstract

HIGH-SOLIDS ANAEROBIC DIGESTION MODEL

ADM1 Based Model

Hypotheses

1) Homogenized Reactors;
2) Porosity and Transport Processes Disregarded;
3) Specific Weights Constant;
4) Biochemical Reactions occur in Water.

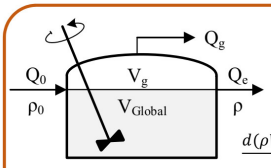

$Q_0 \neq Q_e$

$V_{Global} \neq \text{const.}$

$$\frac{d(\rho V_{Global})}{dt} = \rho_0 Q_0 - \rho Q_e - \sum r_i$$

MODEL SIMULATIONS

Model Verification

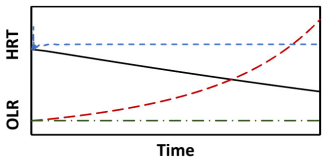

Model Calibration

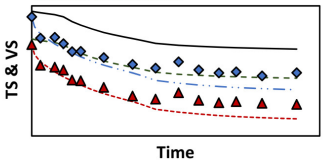

CONCLUSIONS

- Adequate reactor content and TS/VS simulation;
- TS concentration effect needed in HS-AD;
- Further calibration recommended.

POTENTIAL APPLICATION

- Explore Inhibitory and Acidification Mechanisms in HS-AD of OFMSW.

High-Solids Anaerobic Digestion Model for Homogenized Reactors

Vicente Pastor-Poquet [a,b,*], Stefano Papirio [c], Jean-Philippe Steyer [b], Eric Trably [b], Renaud Escudié [b], and Giovanni Esposito [a]

[a] Department of Civil and Mechanical Engineering, University of Cassino and Southern Lazio, via Di Biasio 43, 03043 Cassino (FR), Italy

*Corresponding author. E-mail: vicente.pastor.poquet@gmail.com

[b] LBE, Univ Montpellier, INRA, 102 avenue des Etangs, 11100, Narbonne, France

[c] Department of Civil, Architectural and Environmental Engineering, University of Napoli Federico II, via Claudio 21, 80125 Napoli, Italy

ABSTRACT

During high-solids anaerobic digestion (HS-AD) of the organic fraction of municipal solid waste (OFMSW), an important total solid (TS) removal occurs, leading to the modification of the reactor content mass/volume, in contrast to 'wet' anaerobic digestion (AD). Therefore, HS-AD mathematical simulations need to be approached differently than 'wet' AD simulations. This study aimed to develop a modelling tool based on the anaerobic digestion model 1 (ADM1) capable of simulating the TS and the reactor mass/volume dynamics in the HS-AD of OFMSW. Four hypotheses were used, including the effects of apparent concentrations at high TS. The model simulated adequately HS-AD of OFMSW in batch and continuous mode, particularly the evolution of TS, reactor mass, ammonia and volatile fatty acids. By adequately simulating the reactor content mass/volume and the TS, this model might bring further insight about potentially inhibitory mechanisms (i.e. NH_3 buildup and/or acidification) occurring in HS-AD of OFMSW.

Keywords: High-Solids Anaerobic Digestion; ADM1; Reactor Mass Simulation; Total Solids; Apparent Concentrations.

1 INTRODUCTION

Anaerobic digestion (AD) is a biochemical treatment technology for organic waste valorization yielding a high-methane-content biogas and a partially stabilized organic material with potential applications as soil amendment (Mata-Alvarez 2003). High-solids anaerobic digestion (HS-AD) is a particular case of AD operated at a total solid (TS) content ≥ 10 %, in contrast to 'wet' AD applications (i.e. TS < 10 %) (Abbassi-Guendouz et al. 2012). Thus, HS-AD has the advantage of minimizing the reactor volume, as well as the need for water addition. On the other hand, HS-AD is normally associated with an important reduction of the total (TS) and volatile (VS) solid content, during the biological degradation of the organic matter. For example, HS-AD of the organic fraction of municipal solid waste (OFMSW) might lead to a TS removal of 30 - 80 % (Cecchi et al. 2002, Mata-Alvarez 2003, Pavan et al. 2000). However, some drawbacks limit the applicability of HS-AD as, for example, the reduced kinetics expected as a consequence of the hampered mass transfer, and the high risk of acidification due to organic overloading (Benbelkacem et al. 2015, De Baere 2000). Among the solid wastes used in HS-AD, the OFMSW is particularly suited for anaerobic treatment due to its elevated TS content (i.e. 25 - 30 %), biodegradation potential and possibility to recover nutrients (i.e. nitrogen and phosphorous) from its composition (De Baere and Mattheeuws 2013, Mata-Alvarez 2003). However, HS-AD of OFMSW is normally associated with a high risk of inhibition due to the high protein content, leading to free ammonia nitrogen (NH_3), as one of the most important inhibitors (Chen et al. 2008, Kayhanian 1999, Rajagopal et al. 2013).

Understanding the biochemical and physicochemical dynamics in HS-AD is crucial to ease the design and operation of HS-AD reactors, minimizing the risk of

acidification/inhibition. Particularly important is the knowledge about the interactions between the main four phases – microorganisms, solids, liquids and gases – in HS-AD, since it might allow to increase the waste treatment capabilities and methane yield (Mata-Alvarez 2003, Vavilin et al. 2004, Xu et al. 2015). In this line, an adapted mathematical model is required for the operational analysis and technology development of HS-AD, as some of the main applications for 'wet' AD of the anaerobic digestion model No.1 (ADM1) (Batstone 2006, Batstone et al. 2002, Batstone et al. 2015, Xu et al. 2015).

ADM1 is a structured model gathering together the main biochemical and physicochemical processes of AD (Batstone et al. 2002, Batstone et al. 2015). Biochemical processes include the disintegration, hydrolysis, acidogenesis, acetogenesis and methanogenesis of complex substrates composed of carbohydrates, proteins and lipids in chemical oxygen demand (COD) units. Physicochemical processes include the gas transfer and the equilibrium of the ionic species of the main inorganic compounds in AD (i.e. CO_2 and NH_3). However, the CSTR implementation of ADM1 was primarily conceived for 'wet' AD applications (i.e. TS << 10 %), while a more complex hydraulic and particulate component modeling is required for HS-AD (Batstone et al. 2002, Batstone et al. 2015, Xu et al. 2015). Thus, modelling HS-AD might be particularly challenging due to the intrinsic complexity of the process (Batstone et al. 2015, Mata-Alvarez et al. 2000, Vavilin et al. 2004, Xu et al. 2015). For example, the (semi-)solid matrix might define the soluble/gaseous transport processes, as well as the capabilities of anaerobic biomass to access the substrates (Bollon et al. 2013, Vavilin and Angelidaki 2005).

The mass balance modification, regarding the continuously stirred tank reactor (CSTR) implementation of ADM1 (Batstone et al. 2002), is required to account for the reactor content mass (M_{Global}) removal and the specific weight (ρ_{Global}) dynamics in HS-AD (Batstone et al. 2015, Kayhanian and Hardy 1994, Richards et al. 1991, Vavilin et al. 2004). Noteworthy, the reactor content volume (V_{Global}) might describe important fluctuations during HS-AD, depending mainly on the substrate TS and biodegradability, in contrast to 'wet' AD. Furthermore, a given degree of gaseous porosity (ϵ) might be present in the HS-AD matrix, particularly at TS contents $\geq$ 25 % (Batstone et al. 2015, Benbelkacem et al. 2013, Bollon et al. 2013, Vavilin et al. 2003). ADM1 was originally expressed in volumetric units (i.e. kg COD/m^3). Meanwhile, the most common measurements in HS-AD are normally expressed in mass units (i.e. kg COD/kg), since accounting for the specific weight of (semi-)solid samples – but also the specific weight dynamics in HS-AD – involves the complexity of the analytical techniques (Benbelkacem et al. 2013, Bollon et al. 2013, Kayhanian and Tchobanoglous 1996). For example, the specific weight of a (semi-)solid sample can be approximated by the use of a water pycnometer, where the sample must be appropriately pretreated (i.e. dried/ground), the distilled water fully degassed and analyses performed under temperature-controlled conditions (ASTM 2002). With all the above, HS-AD simulations need to be approached differently than in 'wet' AD, where ρ_{Global} and V_{Global} are normally assumed constant, as summarized in Figure 1.

This study aimed at developing a mathematical tool based on the ADM1 biochemical framework, capable of simulating the solids and reactor content mass/volume dynamics in HS-AD of OFMSW, including the interrelationship between TS (and VS) removal and biogas production. By simulating adequately the global mass/volume and TS

dynamics, the presented model might serve as a link between 'wet' AD and HS-AD, while it might help to explore potential inhibitory/acidification mechanisms occurring during HS-AD of OFMSW. Meanwhile, the proposed model was aimed to be as general as possible, since different HS-AD applications (i.e. organic substrate and/or reactor configuration) could be simulated, provided that the main hypotheses presented in the methodology section are fulfilled. Furthermore, the eventual model user is encouraged to further calibrate the model parameters and/or modify the model structure, in order to adapt the HS-AD model for any specific need.

2 MATERIALS AND METHODS

2.1 High-Solids Model Implementation

The main basis for the dynamic model presented in this study was ADM1 (Batstone et al. 2002), including the modifications suggested by Blumensaat and Keller (2005) for closing nitrogen and carbon balances. The simulation of the HS-AD of OFMSW required four preliminary hypotheses in order to reduce the complexity of the model. Firstly, HS-AD was assumed to take place in a homogenized (i.e. completely mixed) reactor [Hypothesis 1]. Secondly, the effect of porosity and transport processes was assumed to be negligible [Hypothesis 2]. Then, the specific weight of solids and solvent was considered constant [Hypothesis 3]. Finally, the biochemical reactions were assumed to occur predominantly in water [Hypothesis 4].

With these hypotheses, ADM1 required some particular modifications in order to simulate the TS and mass/volume dynamics in HS-AD, while allowing the calibration of the proposed model. The main modifications implemented in ADM1 in order to simulate HS-AD were the inclusion of mass balances modifying the reactor mass and

126 volume (needed to account for the organic solid removal in HS-AD) and the inclusion
127 of apparent concentrations (as a link between 'wet' and high-solids applications).
128
129 **2.1.1 Mass Balances in High-Solid Anaerobic Digestion Reactors**
130 The simulation of the reactor mass and TS/VS content of homogenized HS-AD reactors
131 required the implementation of the global (M_{Global}) [Equation 1], solid material (M_{Solids})
132 [Equation 2], liquid-solvent content ($M_{Solvent}$) [Equation 3] and inert material (M_{Inerts})
133 [Equation 4] mass balances. In this study, the solvent was considered as only water,
134 while the solid material included all the organic and inorganic compounds (i.e.
135 particulates and soluble compounds, VFA, microorganisms) inside the reactor, except
136 water. In mass balances, the mass content (M_i) – global or partial – dynamics were
137 related to the corresponding mass fluxes (m_i), particularly the gases flowing out of the
138 reactor as a consequence of methanogenesis. The implementation of reactor mass
139 balances is crucial in HS-AD, since it accounts for the importance of mass and water
140 removal due to biogas production, in contrast to 'wet' AD (Henze et al. 1997,
141 Kayhanian and Tchobanoglous 1996, Richards et al. 1991).

$$\frac{dM_{Global}}{dt} = m_{Influent,Global} - m_{Effluent,Global} - m_{Biogas} \quad (1)$$

$$\frac{dM_{Solids}}{dt} = m_{Influent,Solids} - m_{Effluent,Solids} - (m_{Biogas} - m_{Vapor}) \quad (2)$$

$$\frac{dM_{Solvent}}{dt} = m_{Influent,Solvent} - m_{Effluent,Solvent} - m_{Vapor} \quad (3)$$

$$\frac{dM_{Inerts}}{dt} = m_{Influent,Inerts} - m_{Effluent,Inerts} \quad (4)$$

142
143 The biogas (m_{Biogas}) [Equation 5] and vapor (m_{Vapor}) [Equation 6] outflows in the mass
144 balances were calculated from the volumetric biogas flow (Q_g), obtained as shown in

145 the CSTR implementation of ADM1 (Batstone et al. 2002), by using the molar gas
146 composition (x_i) and the molecular weight (Mr_i) of each gaseous compound in the gas
147 phase. The biogas was assumed to be composed of CH_4, CO_2, H_2, H_2O and NH_3. The
148 reactor headspace was assumed to be vapor saturated, being vapor pressure (P_v)
149 expressed as a function of temperature (T). On the other hand, an inert gas was added to
150 account for the initial flushing in AD experiments (i.e. by N_2), assuming for it a
151 negligible liquid solubility. Importantly, the inert gas was not included in m_{Biogas}
152 calculations. Once knowing the M_{Global}, M_{Solids} and M_{Inerts}, the TS and VS contents were
153 approximated in dynamic mode by using the corresponding definition (EPA 2001)
154 [Equations 7 & 8]. Noteworthy, TS and VS in the proposed model were dimensionless
155 (i.e. kg Solids/kg Total), varying from 0 to 1.

$$m_{Biogas} = \frac{P_T Q_g}{RT} \sum x_i Mr_i \quad (5)$$

$$m_{Vapor} = \frac{P_v Q_g}{RT} Mr_{H2O} \quad (6)$$

$$TS = \frac{M_{Solids}}{M_{Global}} \quad (7)$$

$$VS = \frac{M_{Solids} - M_{Inerts}}{M_{Global}} \quad (8)$$

156

157 The liquid-gas transfer of gaseous species in the CSTR implementation of ADM1
158 depends on the ratio between the reactor content volume (V_{Global}; 'V_{liq}' in ADM1) and
159 the gas volume (V_g), while their sum yields the design/overall reactor volume ($V_{Reactor}$)
160 (Batstone et al. 2002). Thus, since a considerable reduction of V_{Global} – alongside M_{Global}
161 removal – can occur in HS-AD associated with methanogenesis, the reactor volume was
162 approximated by the specific weigh of the reactor content (ρ_{Global}). Importantly, ρ_{Global}
163 varies also in HS-AD, as it gathers together the individual dynamics of all the mass

compounds in the system (Kayhanian and Tchobanoglous 1996). Therefore, to simulate ρ_{Global}, it is necessary to know the specific weight of all the materials within HS-AD (ρ_i), but also their corresponding mass fraction (m_i) [Equation 9]. For simplicity, the simulations in this study used a common specific weight for all the solid compounds (ρ_{Solids}) and a solvent specific weight ($\rho_{Solvent}$). With these simplifications, the V_{Global} dynamics could be approximated with Equation 10.

$$\frac{1}{\rho_{Global}} = \sum_i \frac{m_i}{\rho_i} \quad (9)$$

$$\frac{dV_{Global}}{dt} = \frac{1}{\rho_{Solids}} \cdot \frac{dM_{Solids}}{dt} + \frac{1}{\rho_{Solvent}} \cdot \frac{dM_{Solvent}}{dt} \quad (10)$$

The distinction between mass and volume in the proposed model for homogenized HS-AD reactors permitted the use of ADM1 volumetric units (i.e. kmol/m^3), while implementing the different influent and effluent mass and/or volumetric flows when operating HS-AD in (semi-)continuous mode. Finally, for illustrative purposes only, an adaptive volumetric effluent ($Q_{Effluent}$) was added to the model – in terms of a proportional controller – to maintain V_{Global} if required. This strategy permitted to compensate for the potential organic mass removal in HS-AD and, therefore, to stabilize the HS-AD system, as further discussed in section 3.1. A schematic diagram of the HS-AD model implementation for homogenized reactors is shown in Figure 2.

2.1.2 Apparent Concentrations – Soluble Species Recalculation

The (soluble) apparent concentrations ($S_{T,i,App}$) were used in the HS-AD model biochemistry and physicochemistry to reproduce the effect of high TS in HS-AD, in contrast to 'wet' AD. This modification was related to the assumption that the main biochemical reactions might occur predominantly in the presence of water (Hypothesis

186 4). Similarly, the apparent concentrations served to link the global (i.e. kmol/kg Total)
187 and liquid fraction (i.e. kmol/kg Solvent) measurements in HS-AD. The apparent
188 concentrations were calculated for all the soluble species of ADM1 using TS, ρ_{Global} and
189 $\rho_{Solvent}$ [Equation 11]. Importantly, the long chain fatty acids (LCFA, S_{fa}) were not
190 considered as soluble in HS-AD, due to their highly non-polar nature and reduced
191 solubility in water (i.e. palmitic acid solubility = 1.2 mg/L at 60 ºC). With this approach,
192 the proposed model simulates the mass balance of dynamic variables ($C_{T,i}$) – either
193 particulate ($X_{T,i}$) or soluble ($S_{T,i}$) – as a function of V_{Global} (i.e. kmol/m^3 Total)
194 [Equation 12], while the apparent concentrations ($S_{T,i,App}$) (i.e. kmol/m^3 Solvent) were
195 used only for the soluble species included in the biochemical and physicochemical rates
196 of ADM1 ($r_{i,ADM1}$) (i.e. uptake of acetate). It is important to mention that Equation 12 is
197 the mass balance of an individual component in AD and, therefore, should be based in
198 the chain rule in order to account for the V_{Global} dynamics, in contrast to the CSTR
199 implementation of ADM1 (Batstone et al. 2002). On the other hand, it should be noted
200 that the effect of apparent concentrations becomes negligible at low TS contents (i.e. TS
201 < 5 %) with ρ_{Global} tending to $\rho_{Solvent}$, as $S_{T,i,App}$ progressively approaches to $S_{T,i}$ in these
202 conditions. With all the above, the sole implementation of the HS-AD mass balances
203 and the use of apparent concentrations in this study might allow to simulate indistinctly
204 'wet' AD and HS-AD conditions, and/or the transition between these two AD regimes,
205 for example, during a prolonged HS-AD operation.

$$S_{T,i,App}\left(\frac{kg\ or\ kmol}{m^3\ Solvent}\right) = \frac{S_{T,i}\left(\frac{kg\ COD\ or\ kmol}{m^3\ Total}\right)}{(1-TS)\left(\frac{kg\ Solvent}{kg\ Total}\right)} \cdot \frac{\rho_{Solvent}\left(\frac{kg\ Solvent}{m^3\ Solvent}\right)}{\rho_{Global}\left(\frac{kg\ Total}{m^3\ Total}\right)} \quad (11)$$

$$\frac{dC_{T,i}}{dt} = \frac{1}{V_{Global}} \cdot \left(Q_{Influent} \cdot C_{T,0} - \frac{m_{Effluent}}{\rho_{Global}} \cdot C_{T,i}\right) + \sum r_{i,ADM1} - \frac{C_{T,i}}{V_{Global}} \cdot \frac{dV_{Global}}{dt} \quad (12)$$

206

207 **2.1.3 Kinetic Rates**

208 The ADM1 biochemical rates and inhibitions were used for the verification of the
209 model implementation according to the protocol proposed by Rosén and Jeppsson
210 (2006). The model verification aimed to test/assess the ADM1 implementation (code)
211 alongside the adequate mathematical solution of the mass balances, determining the TS
212 and organic removal both in 'wet' and high-solids AD applications. On the other hand,
213 a slightly different set of biochemical rates was used for HS-AD model calibration.
214 Thus, calibration aimed to test/assess the HS-AD model performance under real
215 experimental conditions. The biochemical kinetics used in this study are shown in Table
216 1.

217 The biochemical rates used in the HS-AD model were associated with the inhibitory
218 functions as originally proposed in ADM1 (Batstone et al. 2002, Rosén and Jeppsson
219 2006) [Equations 13 to 16]. However, all the soluble species terms included in the HS-
220 AD biochemical rates – excluding S_{fa} – were expressed in terms of apparent
221 concentrations, as mentioned in section 2.1.2.

$$I_{in} = \frac{S_{in,App}}{K_{S,Sin} + S_{in,App}} \quad (13)$$

$$I_{h2} = \frac{K_{i,Sh2}}{K_{i,Sh2} + S_{h2,App}} \quad (14)$$

$$I_{pH} = \frac{{K_{pH}}^{N_{pH}}}{{K_{pH}}^{N_{pH}} + {S_{proton}}^{N_{pH}}} \quad (15)$$

$$I_{nh3} = \frac{K_{i,Snh3}}{K_{i,Snh3} + S_{nh3,App}} \quad (16)$$

222

223 Regarding the HS-AD model implementation used for calibration [Table 1], the valerate
224 uptake was assumed to be carried out by valerate degraders (X_{c5}), instead of butyrate
225 and valerate being both degraded by butyrate degraders (X_{c4}), as proposed in ADM1
226 (Batstone et al. 2002). This last modification was used to account for the different
227 dynamics observed for butyrate and valerate uptake in the experimental data. The
228 valerate parameters and rates were maintained as in the original thermophilic (55 ºC)
229 implementation of ADM1, though the X_{c5} decay was included in the biochemical
230 matrix. On the other hand, the microbial decay was assumed to yield particulate
231 substances (i.e. carbohydrates and proteins) directly, avoiding the use of a composite
232 material (X_c) and the associated disintegration kinetics (Batstone et al. 2015). The
233 biomass decay COD fractioning (i.e. $f_{ch,xc}$) was maintained as proposed by Rosén and
234 Jeppsson (2006). However, the inert materials (i.e. S_i and X_i) carbon content (C_i) was
235 modified to 0.0405 kmol C/kg COD in order to close the biomass carbon balance, while
236 the inert nitrogen content (N_i) was modified to 0.0144 kmol N/kg COD to close the
237 biomass nitrogen balance. This last modification permitted to reduce the stiffness and
238 speed up the model simulations in this study.
239 The degradation of the protein content of an organic waste determines the total
240 ammonia nitrogen (TAN, S_{in}) in HS-AD (Kayhanian 1999). In this line, the nitrogen
241 balance has to be closed for the microorganisms in ADM1, while adding complex
242 substrates implies the fulfilment of the corresponding nitrogen balances. For this study,
243 two nitrogen balances were used for the biomass and substrate as shown in Equations
244 17 and 18, respectively, assuming a common nitrogen content for proteins/amino acids
245 (N_{aa}). With this approach, two new inert variables ($S_{i,subs}$ and $X_{i,subs}$) were added to

ADM1 in order to calibrate the initial protein content (X_{pr}) and/or the experimental TAN dynamics. The nitrogen balance for biomass [Equation 17] remained closed as mentioned before, while the protein fraction of the substrate-inoculum mixture ($f_{pr,subs}$) could be adjusted by calibrating the inert nitrogen content of the substrate-inoculum mixture ($N_{i,subs}$), since all the remaining variables in the nitrogen balance (N_{subs}, $f_{si,subs}$ and $f_{xi,subs}$) [Equation 18] could be obtained experimentally. For example, the anaerobic biodegradability (i.e. $COD_{removed}/COD_{substrate}$) of an organic substrate is equivalent to 1 - ($f_{si,subs}$ + $f_{xi,subs}$), while the global nitrogen content of the substrate-inoculum mixture (N_{subs}) is the quotient between the total Kjeldahl nitrogen (TKN) and COD (i.e. $TKN_{substrate}/COD_{substrate}$).

$$N_{bac} = f_{pr,xc} \cdot N_{aa} + (f_{si,xc} + f_{xi,xc}) \cdot N_i \quad (17)$$

$$N_{subs} = f_{pr,subs} \cdot N_{aa} + \left(f_{si,subs} + f_{xi,subs}\right) \cdot N_{i,subs} \quad (18)$$

2.2 Verification of the Model Implementation

The proposed model implementation was verified for 'wet' AD according to Rosén and Jeppsson (2006). Similarly, the model was further tested for HS-AD conditions. In total, four different verification scenarios were simulated: A) 'wet' AD using the ADM1 implementation of Rosén and Jeppsson (2006); B) 'wet' AD using the HS-AD model implementation with a constant $Q_{Effluent}$; C) HS-AD using the HS-AD model and constant $Q_{Effluent}$; and D) HS-AD considering the HS-AD model with an adaptive $Q_{Effluent}$. The HS-AD model was coded in MATLAB® R2017a. The equation resolution was the ode15s; a variable-step, variable-order solver based on the numerical differentiation formulas of orders 1 to 5. The influent conditions used for model verification are shown in Table 2.

Noteworthy, the only difference between the influent conditions during simulations A and B was the introduction of the TS, VS and ρ_{Global} of the substrate in the last case [Table 2], permitting to excite the high-solids module of the proposed HS-AD model, in contrast to the CSTR implementation of ADM1. On the other hand, for illustrative purposes only, a high-solids substrate was included using a different carbohydrate (X_{ch}) and particulate inert (X_i) content, but also TS, VS and ρ_{Global}, for simulations C and D [Table 2]. Thus, the high TS content of the influent conditions (i.e. 25 %), associated predominantly with X_{ch} and X_i, permitted to test the model under HS-AD operation, while avoiding potential inhibitory states due to NH_3 accumulation.

During the verification of the model implementation, all the ADM1 parameters were used as proposed by Rosén and Jeppsson (2006) for mesophilic (35 ºC) AD operation, though the original hydrolysis constant for carbohydrates ($k_{h,ch}$) had to be reduced to 0.10 days in the HS-AD verification only (simulations C and D), in order to avoid reactor overloading and acidification (i.e. pH $\leq$ 6.0) during the initial days of simulation. 200 days of 'wet' AD or HS-AD operation were simulated for each verification scenario. The organic loading rate (OLR) was evaluated as the daily substrate addition in COD units divided by V_{Global}, while the hydraulic retention time (HRT) was evaluated as the quotient between V_{Global} and $Q_{Effluent}$.

2.3 Experimental Data and Data Recalculation

The experimental data used to calibrate the HS-AD model consisted in a batch-sacrifice test fed with dried OFMSW and centrifuged inoculum at TS of 15 % operated under thermophilic (55 ºC) conditions. In the sacrifice test, 15 replicates were implemented in 250 mL serum bottles. Thus, after measuring the biogas volume and composition, a

292 single replicate was opened, and the HS-AD content thoroughly analyzed for the main
293 physicochemical variables. The experimental results included the TS, VS, ρ_{Global}, COD,
294 TKN, TAN, pH, volatile fatty acids (VFA; valeric, butyric, propionic and acetic acids),
295 mono-valent ions (Na^+, K^+ and Cl^-), biogas composition (CH_4, CO_2 and H_2) and
296 methane yield. The serum bottles were agitated only on those days when the biogas
297 production was measured. Further information about the experimental setup, substrate,
298 inoculum and physicochemical analyses is presented as Supplementary Information.
299 Importantly, an experimental bias might exist on TS measurements whether volatile
300 compounds (i.e. NH_3, CO_2 and VFA) are lost when drying at 105 ºC (Angelidaki et al.
301 2009, EPA 2001). For this study, the mass of volatile substances at 105 ºC ($M_{Volatiles}$)
302 was assumed to be equivalent to the total mass of VFA (S_{ac}, S_{pro}, S_{bu} and S_{va}), TAN (S_{in})
303 and inorganic carbon (S_{ic}) [Equation 19]. Thus, the simulated TS and VS were
304 recalculated *a posteriori* (TS_{Recalc} and VS_{Recalc}) [Equation 20 and 21] in order to
305 compare them with the experimental values.

$$M_{Volatiles} = (S_{ac} \cdot \frac{60}{64} + S_{pro} \cdot \frac{74}{112} + S_{bu} \cdot \frac{88}{160} + S_{va} \cdot \frac{102}{208} + S_{in} \cdot 17 + S_{ic} \cdot 44) \cdot V_{Global} \quad (19)$$

$$TS_{Recalc} = \frac{M_{Solids} - M_{Volatiles}}{M_{Global}} \quad (20)$$

$$VS_{Recalc} = \frac{M_{Solids} - M_{Inerts} - M_{Volatiles}}{M_{Global}} \quad (21)$$

306

307 **2.4 Model Calibration**

308 The calibration of some of the main biochemical parameters in this study aimed to
309 obtain the best fitting with the experimental data for a homogenized HS-AD laboratory-
310 scale reactor, in order to assess the correct simulations of the TS and reactor content
311 dynamics. The model calibration was carried out by trial and error, mainly for the

hydrolysis (i.e. $k_{h,ch}$) and maximum growth rate (i.e. $k_{m,su}$) constants, aiming to maintain as close as possible the parameters proposed for thermophilic (55 ºC) AD in ADM1 (Batstone et al. 2002). Noteworthy, the initial composition (i.e. S_{ac}, S_{in}) was chosen based on the evaluation of the experimental data available (i.e. VFA, TAN), while all the initial microorganisms concentrations (i.e. X_{ac}, X_{su}) were calibrated also by trial and error, alongside the main biochemical parameters, as further discussed in section 3.2.1.

3 RESULTS AND DISCUSSION

3.1 Model Implementation Verification

3.1.1 'Wet' AD Verification

The model verification for 'wet' AD operating in a CSTR (simulation A) showed minimal differences (i.e. 4^{th}-5^{th} significant digit) compared to the results suggested by Rosén and Jeppsson (2006) [Table 3], being these differences likely associated with the slightly different equation resolution method used [U. Jeppsson, Personal Communication]. Importantly, when using the HS-AD model implementation for 'wet' AD (simulation B), the results were again very close to the original 'wet' ADM1 verification, though some differences could be observed for all the dynamic variables [Table 3]. For example, the acetic acid (S_{ac}) predicted with the HS-AD model implementation (simulation B) was around 39 % higher than that in the original ADM1 (simulation A). The TS concentration effect of apparent concentrations might define some differences among all the soluble species during 'wet' AD (i.e. S_{ac}, $S_{h2,}$ S_{nh3}), though the apparent concentrations effect in 'wet' applications was relatively small in simulation B due to the low TS content (i.e. < 5 %) [Equation 11].

335 It is important to mention that the differences between simulations A and B were related
336 to the fact that the 'wet' AD simulation using the HS-AD model (simulation B) did not
337 reach steady-state. Thus, a steady-state operation in simulation B was not reached even
338 after 200 days, particularly due to the implementation of a common volumetric
339 influent/effluent (i.e. $Q_{Influent} = Q_{Effluent}$). In this line, simulation B showed an overall
340 37 % reduction in the TS content after 200 days, as well as a 13 % reduction in the
341 V_{Global} (but also HRT), and a 0.5 % reduction in ρ_{Global} [Table 3]. Therefore, a daily-
342 averaged 0.06 % V_{Global} modification occurred in 'wet' AD using the HS-AD model,
343 which might be considered negligible for short operation periods, but increasingly
344 important for longer operation (Henze et al. 1997, Richards et al. 1991). The
345 progressive reduction of the HRT during simulation B led to a proportional increase in
346 the OLR from 2.85 to 3.27 kg COD/$m^3 \cdot d$ [Figure 3a], explaining the differences
347 between simulations A and B (i.e. S_{ac}) mentioned before. Interestingly, the reduction in
348 ρ_{Global} (i.e. 0.994 kg/L) below $\rho_{Solvent}$ (i.e. 1.000 kg/L) suggests that the influent
349 conditions (i.e. $\rho_{Global0} = \rho_{Solvent}$) and/or the model simplifications (i.e. ρ_{Solids} = const.)
350 required further testing.
351 The specific weight of a complex sample (ρ_{Global}) depends on all the compounds
352 involved [Equation 9]. Since the measurement of all the variables ρ_i in an AD sample is
353 rarely available, the ρ_i of each compound needs to be known/assumed for simulations.
354 In this line, the specific weight of a sample solid fraction (ρ_{Solids}) can be approximated
355 by knowing the specific weight of the solvent ($\rho_{Solvent}$), though $\rho_{Solvent}$ is again function
356 of all the different compounds in solution, as well as a function of temperature and
357 pressure (Lide 2004). As a preliminary approach, $\rho_{Solvent}$ was assumed to be close to the
358 specific weight (density) of water at 0 ºC and 1 bar (i.e. $\rho_{Solvent}$ = 1 kg/L), since the

359 density of water is 999.84 kg/m^3 at 0 ºC, 993.64 kg/m^3 (0.63 % error) at 35 ºC, and
360 985.19 kg/m^3 (1.48 % error) at 55 ºC (Kell 1975, Lide 2004), thus being approximately
361 constant at any of these temperatures. With this strategy, the specific weights obtained
362 for the overall sample (ρ_{Global}) and/or the solid fraction (ρ_{Solids}) were considered relative
363 regarding the specific weight of solvent ($\rho_{Solvent}$). Meanwhile, $\rho_{Solvent}$ (but also ρ_{Solids})
364 could be set to any value, or modified by any expression (i.e. as a function of
365 temperature), without modifying the structure of the model. Thus, once knowing the
366 $\rho_{Solvent}$, the ρ_{Global} and TS of a (semi-)solid sample, ρ_{Solids} could be approximated by
367 using the mass balance [Equation 9].
368 Previous research indicated that ρ_{Solids} ranges from 1.3 kg/L in lignocellulosic materials
369 to 1.5 kg/L in OFMSW and 2.5 kg/L for inorganic inert solids (i.e. sand). On the other
370 hand, the specific weight of microorganisms is reported between 0.8 and 1.4 kg/L (van
371 Veen and Paul 1979), though this fraction might be a negligible part (i.e. 5 %) of the
372 whole reactor mass content. Therefore, a compromise value of ρ_{Solids} = 1.5 kg/L was
373 chosen for the preliminary model verification/calibration, though further testing must be
374 devoted to this particular variable, since it could influence other aspects of the HS-AD
375 simulations (i.e. V_{Global}), as mentioned before.
376
377 **3.1.2 HS-AD Verification**
378 Regarding the HS-AD model verification with constant $Q_{Effluent}$ (simulation C), the HS-
379 AD simulation did not reach the steady state after 200 days, while longer simulations
380 (i.e. 365 days) yielded reactor acidification (i.e. pH $\leq$ 6.0) – data not shown. This is due
381 to a progressive reduction of V_{Global} in HS-AD when maintaining a volumetric outflow
382 equal to the volumetric inflow (i.e. $Q_{Influent} = Q_{Effluent}$) (Kayhanian and Tchobanoglous

1996, Richards et al. 1991). Thus, the HRT decreases – and the OLR increases – proportionally to the V_{Global} reduction in HS-AD until the 'washout' of methanogens occurs and the reactor acidifies. For example, a 50 % reduction in HRT was observed with the influent conditions tested in simulation C [Figure 3b], with an approximately daily-averaged V_{Global} reduction of 0.25 %.

Meanwhile, a rapid stabilization of the HS-AD process was obtained when choosing a constant reactor volume as a set point (i.e. $V_{Setpoint} = V_{Global0}$) and recalculating $Q_{Effluent}$ [Table 3 and Figure 3b]. Noteworthy, the $Q_{Effluent}$ recalculation operation yielded a reduction of around 5.6 % of the steady-state value regarding $Q_{Influent}$, and a 24 % TS removal compared to the substrate TS (i.e. from 25 to 19 %). These results condense the importance of reducing the effluent compared to the influent (i.e. $Q_{Influent} > Q_{Effluent}$) to reach steady-state HS-AD, in order to compensate the organic removal by methanogenesis (Kayhanian and Hardy 1994, Kayhanian and Tchobanoglous 1996, Richards et al. 1991). Furthermore, the use of apparent concentrations might be also crucial for HS-AD simulations, since practically all the biochemical rates were affected (i.e. speeded-up/slowed-down) by the TS concentration effect on soluble substrates (i.e. S_{ac}) and/or inhibitors (i.e. S_{nh3}) [Table 1]. For example, a 26 % increase in all the soluble concentrations (i.e. S_{su} and S_{h2}) was obtained by the tested HS-AD conditions in steady-state operation – data not shown.

The water/solvent in this study was assumed to be conservative, since the same water entering leaves the system as a liquid effluent ($m_{Effluent,Solvent}$) or vapor (m_{Vapor}), but is not produced/consumed. Importantly, production/consumption of water in the biochemical processes (i.e. hydrolysis, methanogenesis) might occur, linking Equations 2 and 3. However, the production/consumption of water is tightly linked to the

stoichiometry of all the reactions occurring in HS-AD, while the stoichiometry of all the biochemical reactions in ADM1 requires further development (De Gracia et al. 2006, Kleerebezem and van Loosdrecht 2006, Rodríguez et al. 2006). Therefore, using Equations 1 to 4 is a reasonable hypothesis that can be modified, once the global stoichiometry of HS-AD is well-defined. In this last case, the Petersen matrix originally proposed for ADM1 would need to account for water as another dynamic variable. For example, De Gracia et al. (2006) included water (i.e. S_{h2o}) in the Petersen matrix of ADM1, though the AD stoichiometry was partially assumed (i.e. elemental composition). Furthermore, in order to use Equations 1 to 4 in this study, it was also assumed that the organic solid destruction only proceeds when biogas production occurs. In other words, whether hydrolysis, acidogenesis and/or acetogenesis occur, but not biogas production (i.e. CH_4, CO_2 and/or H_2), complex substrates (i.e. carbohydrates) are just transformed into more simple substrates (i.e. sugars, VFA), being both of them jointly included in the term $m_{Effluent,Solids}$. With these two last assumptions, the hydrolysis to acidogenesis steps were not included in Equations 1 to 4. However, the mass volatile compounds at 105 ºC ($M_{Volatiles}$) needed to be accounted in the TS and VS calculations, as shown in Equations 19 to 21.

Due to the considerably higher COD of the influent conditions [Table 2], the OLR was around 7 times higher for HS-AD than for 'wet' AD simulations [Table 3], which directly relates to the higher chances of HS-AD acidification, and the necessity to reduce considerably the $k_{h,ch}$ for HS-AD simulations. In either case, HS-AD experimental data are required to calibrate biochemical parameters (i.e. $k_{h,ch}$).

3.2 Model Calibration

3.2.1 Comparison Between Simulated and Experimental Values

The HS-AD simulation of OFMSW in batch conditions at 15 % TS closely matched all the experimental variables [Figure 4], though slight disagreements were also observed between the experimental data and the simulated values. The initial conditions and modified parameters used are shown in Tables 2 and 4, respectively. Firstly, the cumulative methane production was 830 NmL CH_4 [Figure 4a], coinciding to that obtained experimentally, while the biogas composition was also well simulated – data not shown. Importantly, the overall biogas production was associated with 1.7 g M_{Global} removal (i.e. 4.6 %), in agreement with the 1.5 - 2.0 g that could have been removed according to the experimental biogas flow/composition. Noteworthy, the simulation suggested that ρ_{Global} was reduced from 1078 to 1064 kg/m^3 (i.e. 1.2 % reduction) along the whole experimental period (data not shown), though the ρ_{Global} modification should be further validated with experimental data, as discussed before. The M_{Global} and ρ_{Global} modification yielded a V_{Global} reduction of 3.5 % – data not shown.

The initial composition in the batch experiment [Table 2] was based on the availability of experimental data (i.e. COD, TS and CH_4 yield), but also on a reasoned assessment of the substrate and/or inoculum composition. For example, the protein content of the substrate/inoculum mixture (i.e. $X_{pr} + S_{aa}$) was adjusted according to the nitrogen content of proteins and amino acids (N_{aa}) [Table 4] and the inert materials (i.e. $X_i + S_i$) to simulate the TAN (S_{in}) dynamics, as mentioned in section 2.1.3. Unfortunately, apart from the CH_4 yield and COD of the initial mixture, no data were available regarding the remaining complex substances (i.e. particulates) involved in the biochemical framework of the model. Therefore, the distinction between the initial carbohydrate/sugars (X_{ch}/S_{su})

454 and lipids/LCFA (X_g/S_{fa}) had to be tuned alongside the biochemical parameters to
455 simulate the initial days of the batch setup.
456 During the initial 20 days of experiment, pH was observed to drop from 7.3 to 6.3 –
457 data not shown – due to VFA accumulation [Figure 4b]. Thus, the initial VFA and pH
458 dynamics were simulated by a plausible set of microorganism concentrations,
459 hydrolysis constants and initial substrate/inoculum fractionation [Tables 2 and 4]. The
460 initial microbial concentrations are crucial in the simulation of AD batch experiments,
461 though they are normally unknown due to the difficulties for measuring the populations
462 involved (Donoso-Bravo et al. 2011, Flotats et al. 2010). Importantly, the hydrolysis
463 constants (k_h) were considerably reduced compared to the original values proposed in
464 ADM1 for thermophilic (55 ºC) operation (i.e. $k_{h,ch}$ = 0.05 d^{-1} vs. 10 d^{-1}, respectively),
465 though the calibrated values were in accordance with reported hydrolysis rates for
466 simulation of OFMSW (Batstone et al. 2002, Kayhanian 1995, Mata-Alvarez 2003,
467 Vavilin and Angelidaki 2005).
468 In order to obtain the best fitting between the simulated and experimental VFA
469 dynamics from day 20, the maximum growth rate (k_m) of some microbial populations
470 was also considerably reduced. For example, the maximum growth rate of propionate
471 degraders ($k_{m,pro}$) was reduced to 1 d^{-1}, in contrast to the 20 d^{-1} proposed by ADM1 for
472 thermophilic (55 ºC) operation [Table 4]. Noteworthy, the extremely low k_m used for
473 model calibration, in contrast to the original values of ADM1, might be suggesting that
474 some inhibition in the VFA uptake was occurring in the experiment. Thus, NH_3 reached
475 particularly high contents in the reactor (i.e. 0.16 mol N/kg) [Figure 4c] mainly due to
476 the high pH observed (i.e. ≥ 8.0), while NH_3 is a well-known inhibitor of acetoclastic
477 and hydrogenotrophic methanogens (Angelidaki and Ahring 1993, Gallert and Winter

1997, Jokela and Rintala 2003). In this line, the implementation of reversible NH_3 inhibition [Equation 16] in hydrogen uptake could match adequately all the VFA, since valerate and propionate degraders are inhibited by H_2 buildup in ADM1 (Batstone et al. 2002). However, this last strategy led to H_2 accumulation in the gas phase (i.e. 2 - 5 %, data not shown), though no H_2 was detected experimentally. Therefore, all the VFA-degrading populations might be affected in some degree by NH_3 accumulation, as suggested by Poggi-Varaldo et al. (1997).

The model suggested a 5 - 15 % difference between the simulated and experimental TS and VS contents, despite the experimental trends were well approximated in both cases [Figure 4d]. Therefore, since the simulated M_{Global}, CH_4 yield and COD showed good simulations, an experimental bias was suspected in the experimental TS/VS measurement. Noteworthy, the recalculated TS and VS [Equations 19 to 21] improved considerably the matching of the TS and VS simulations with the values observed experimentally, though some differences were also observed from day 20 onwards. Meanwhile, the TS and VS recalculation is supported by the fact that some organic material (i.e. VFA), ammonia nitrogen (i.e. NH_3) and/or inorganic carbon (i.e. CO_2) might volatilize when drying the samples at 105 ºC for prolonged periods of time (i.e. 24 h) (Angelidaki et al. 2009, EPA 2001). With all the above, the observed differences between the TS and VS recalculated and experimental values [Figure 4d] were likely related to the differences in the propionate and valerate simulations [Figure 4b] during the same period. Therefore, the model calibration might require further improvement as also discussed in next section.

3.2.2 Need for Further Calibration

The model calibration in this study was aimed to be minimal because of: 1) the complexity of HS-AD vs. the assumptions taken (i.e. homogenized reactor); 2) the little data available regarding solids mass dynamics (i.e. TS/VS); 3) the high number of biochemical parameters involved (i.e. > 10); and 4) the 'strong' interrelationship between parameters and the initial conditions in structured AD models (Batstone et al. 2015, Donoso-Bravo et al. 2011, Flotats et al. 2010, Vanrolleghem et al. 1995). Thus, the calibration in this study was mainly addressed to the simultaneous fitting of the overall dynamics of TS/VS removal, reactor mass, biogas production, VFA and pH, in order to assess the potentiality of the proposed model to simulate a homogenized HS-AD matrix.

The parameter modification compared to ADM1 values [Table 4] was needed to obtain an adequate fitting of the overall set of experimental data for the sacrifice test in this study. Importantly, most of the biochemical parameters modified were within the recommended range suggested in ADM1, with the exception of the maximum propionate and valerate growth rates (i.e. $k_{m,pro}$ and $k_{m,va}$) that could be associated to NH_3 inhibition, as mentioned in section 3.2.1. For example, the lower and upper pH levels for acetate uptake ($pH_{LL,ac}$ and $pH_{UL,ac}$, respectively) might vary around 30 % from the values proposed in ADM1 (i.e. $pH_{LL,ac}$ = 6.0 and $pH_{UL,ac}$ = 7.0) (Batstone et al. 2002). However, it must be highlighted that the implementation of a single experimental dataset was not enough to calibrate a large number of parameters since, for example, different combinations of biochemical parameters and/or initial conditions (i.e. microorganisms) could yield practically the same agreement between experimental and simulated results (Girault et al. 2011, Jablonski and Lukaszewicz 2014, Vanrolleghem et al. 1995, Vavilin et al. 2008). Therefore, more experimental datasets (i.e. laboratory

and/or large scale applications) are needed to refine the calibration of the proposed parameters for HS-AD of OFMSW. Meanwhile, a sensitivity analysis and an adequate parameter optimization strategy might reveal important aspects about the main biochemical and physicochemical processes occurring in HS-AD of OFMSW.

With all the above, the minimal model calibration showed the potentiality of using adequately the mass balances alongside the biochemical framework of ADM1 to simulate HS-AD of OFMSW. Thus, the HS-AD model simulates particularly well the TS, VS, and M_{Global} dynamics of HS-AD, provided the four preliminary hypotheses proposed are fulfilled. Meanwhile, further studies are needed in order to improve the biochemical calibration of the HS-AD model, with the aim to explore the different acidification/inhibitory mechanisms of HS-AD fed with OFMSW. Further calibration will be also helpful to double check the hypotheses used, assess the HS-AD model performance and/or highlight potential areas requiring further model development. Summarizing, the user could calibrate the model parameters and/or readapt the HS-AD model structure as required for any particular HS-AD application.

4 CONCLUSIONS

In this study, a novel ADM1-based model was developed to simulate the solids and reactor mass/volume dynamics of homogenized HS-AD reactors. An adequate mass balance implementation condensed the effects of biogas production on HS-AD mass/volume, being critical to simulate relatively long operations. Apparent concentrations accounted for the TS concentration effect on soluble species. The model was verified for ‘wet’ AD and HS-AD, serving as a link between both operational regimes. The model simulated particularly well HS-AD of OFMSW in batch, including

550 the TS and reactor mass, while further model calibration might serve to assess
551 inhibitory mechanisms in HS-AD of OFMSW.
552
553 **Acknowledgements**
554 This project has received funding from the European Union's Horizon 2020 research
555 and innovation programme under the Marie Sklodowska-Curie grant agreement No.
556 643071. The authors thank Ulf Jeppsson for his inestimable comments when verifying
557 the ADM1 implementation.

558 **REFERENCES**
559
560 Abbassi-Guendouz, A., Brockmann, D., Trably, E., Dumas, C., Delgenes, J.P., Steyer,
561 J.P. and Escudie, R. (2012) Total solids content drives high solid anaerobic
562 digestion via mass transfer limitation. Bioresour. Technol. 111, 55-61.
563 Angelidaki, I. and Ahring, B.K. (1993) Thermophilic anaerobic digestion of livestock
564 waste: the effect of ammonia. Appl. Microbiol. Biotechnol. 38(4), 560–564.
565 Angelidaki, I., Alves, M., Bolzonella, D., Borzacconi, L., Campos, J.L., Guwy, A.J.,
566 Kalyuzhnyi, S., Jenicek, P. and van Lier, J.B. (2009) Defining the biomethane
567 potential (BMP) of solid organic wastes and energy crops: a proposed protocol for
568 batch assays. Water Sci. Technol. 59(5), 927-934.
569 ASTM (2002) D854-02: Standard test methods for specific gravity of soil solids by
570 water pycnometer, ASTM International, American Society for Testing and
571 Materials, United States.
572 Batstone, D.J. (2006) Mathematical modelling of anaerobic reactors treating domestic
573 wastewater: rational criteria for model use. Rev. Environ. Sci. Bio. 5(1), 57-71.
574 Batstone, D.J., Keller, J., Angelidaki, I., Kalyuzhnyi, S.V., Pavlostathis, S.G., Rozzi, A.,
575 Sanders, W.T., Siegrist, H. and Vavilin, V.A. (2002) The IWA Anaerobic
576 Digestion Model No. 1 (ADM1). Water Sci. Technol. 45(10), 65-73.
577 Batstone, D.J., Puyol, D., Flores-Alsina, X. and Rodríguez, J. (2015) Mathematical
578 modelling of anaerobic digestion processes: applications and future needs. Rev.
579 Environ. Sci. Bio. 14(4), 595-613.
580 Benbelkacem, H., Bollon, J., Bayard, R., Escudié, R. and Buffière, P. (2015) Towards
581 optimization of the total solid content in high-solid (dry) municipal solid waste
582 digestion. Chem. Eng. J. 273, 261-267.
583 Benbelkacem, H., Garcia-Bernet, D., Bollon, J., Loisel, D., Bayard, R., Steyer, J.P.,
584 Gourdon, R., Buffiere, P. and Escudie, R. (2013) Liquid mixing and solid
585 segregation in high-solid anaerobic digesters. Bioresour. Technol. 147, 387-394.
586 Blumensaat, F. and Keller, J. (2005) Modelling of two-stage anaerobic digestion using
587 the IWA Anaerobic Digestion Model No. 1 (ADM1). Water Res. 39(1), 171-183.
588 Bollon, J., Benbelkacem, H., Gourdon, R. and Buffière, P. (2013) Measurement of
589 diffusion coefficients in dry anaerobic digestion media. Chem. Eng. Sci. 89, 115-
590 119.
591 Cecchi, F., Pavan, P., Battistoni, P., Bolzonella, D. and Innocenti, L. (2002)
592 Characteristics of the organic fraction of municipal solid wastes in Europe for
593 different sorting strategies and related performances of the anaerobic digestion
594 process, Mérida, Yucatán.
595 Chen, Y., Cheng, J.J. and Creamer, K.S. (2008) Inhibition of anaerobic digestion
596 process: a review. Bioresour. Technol. 99(10), 4044-4064.
597 De Baere, L. (2000) Anaerobic digestion of solid waste: state-of-the-art. Water Sci.
598 Technol. 41(3), 283-290.
599 De Baere, L. and Mattheeuws, B. (2013) Waste Management: Recycling and Recovery.
600 Thomé-Kozmiensky Karl J., T.S. (ed), pp. 517-526.
601 De Gracia, M., Sancho, L., García-Heras, J.L., Vanrolleghem, P. and Ayesa, E. (2006)
602 Mass and charge conservation check in dynamic models: application to the new
603 ADM1 model. Water Sci. Technol. 53(1), 225-240.

604 Donoso-Bravo, A., Mailier, J., Martin, C., Rodriguez, J., Aceves-Lara, C.A. and Vande
605 Wouwer, A. (2011) Model selection, identification and validation in anaerobic
606 digestion: a review. Water Res. 45(17), 5347-5364.
607 EPA (2001) Method 1684. Total, fixed and volatile solids in water, solids, and
608 biosolids., U.S. Environmental Protection Agency (EPA), Washington, DC.
609 Flotats, X., Palatsi, J., Fernandez, B., Colomer, M.A. and Illa, J. (2010) Identifying
610 anaerobic digestion models using simultaneous batch experiments. Environ.
611 Engineer. Manag. J. 9(3), 313-318.
612 Gallert, C. and Winter, J. (1997) Mesophilic and thermophilic anaerobic digestion of
613 source-sorted organic wastes: effect of ammonia on glucose degradation and
614 methane production. Appl. Microbiol. Biotechnol. 48, 405-410.
615 Girault, R., Rousseau, P., Steyer, J.P., Bernet, N. and Béline, F. (2011) Combination of
616 batch experiments with continuous reactor data for ADM1 calibration: application
617 to anaerobic digestion of pig slurry. Water Sci. Technol. 63(11), 2575.
618 Henze, M., Harremoes, P., Jansen, J.l.C. and Arvin, E. (1997) Wastewater treatment.
619 Biological and chemical processes, Springer, Berlin.
620 Jablonski, S.J. and Lukaszewicz, M. (2014) Mathematical modelling of methanogenic
621 reactor start-up: importance of volatile fatty acids degrading population.
622 Bioresour. Technol. 174, 74-80.
623 Jokela, J.P. and Rintala, J. (2003) Anaerobic solubilisation of nitrogen from municipal
624 solid waste (MSW). Rev. Environ. Sci. Bio. 2, 67-77.
625 Kayhanian, M. (1995) Biodegradability of the organic fraction of municipal solid waste
626 in a high-solids anaerobic digester. Waste Manage. Res. 13, 123-136.
627 Kayhanian, M. (1999) Ammonia inhibition in high-solids biogasification: an overview
628 and practical solutions. Environ. Technol. 20(4), 355-365.
629 Kayhanian, M. and Hardy, S. (1994) The impact of four design parameters on the
630 performance of a high-solids anaerobic digestion of municipal solid waste for fuel
631 gas production. Environ. Technol. 15(6), 557-567.
632 Kayhanian, M. and Tchobanoglous, G. (1996) Development of a mathematical model
633 for the simulation of the biodegradation of organic substrates in a high-solids
634 anaerobic digestion. J. Chem. Tech. Biotechnol. 66, 312-322.
635 Kell, G.S. (1975) Density, thermal expansivity, and compressibility of liquid water from
636 0 to 150°C: Correlations and tables for atmospheric pressure and saturation
637 reviewed and expressed on 1968 temperature scale. J. Chem. Eng. Data 20(1), 97-
638 105.
639 Kleerebezem, R. and van Loosdrecht, M.C.M. (2006) Critical analysis of some concepts
640 proposed in ADM1. Water Sci. Technol. 54(4), 51-57.
641 Lide, D.R. (2004) Hanbook of chemistry and physics, CRC Press.
642 Mata-Alvarez, J. (2003) Biomethanization of the organic fraction of municipal solid
643 wastes, IWA Publishing, London, UK.
644 Mata-Alvarez, J., Macé, S. and Llabrés, P. (2000) Anaerobic digestion of organic solid
645 wastes. An overview of research achievements and perspectives. Bioresour.
646 Technol. 74(1), 3-16.
647 Pavan, P., Battistoni, P., Mata-Alvarez, J. and Cecchi, F. (2000) Performance of
648 thermophilic semi-dry anaerobic digestion process changing the feed
649 biodegradability. Water Sci. Technol. 41(3), 75-81.

650 Poggi-Varaldo, H.M., Valdés, L., Esparza-García, F. and Fernández-Villagómez, G.
651 (1997) Solid substrate anaerobic co-digestion of paper mill sludge, biosolids, and
652 municipal solid waste. Water Sci. Technol. 35(2-3), 197-204.
653 Rajagopal, R., Masse, D.I. and Singh, G. (2013) A critical review on inhibition of
654 anaerobic digestion process by excess ammonia. Bioresour. Technol. 143, 632-
655 641.
656 Richards, B.K., Cummings, R.J., White, T.E. and Jewell, W.J. (1991) Methods for
657 kinetic analysis of methane fermentation in high solids biomass digesters.
658 Biomass Bioenergy 1(2), 65-73.
659 Rodríguez, J., Lema, J.M., van Loosdrecht, M.C.M. and Kleerebezem, R. (2006)
660 Variable stoichiometry with thermodynamic control in ADM1. Water Sci.
661 Technol. 54(4), 101-110.
662 Rosén, C. and Jeppsson, U. (2006) Aspects on ADM1 implementation within the BSM2
663 framework., Division of Industrial Electrical Engineering and Automation,
664 Faculty of Engineering, Lund University, Sweden.
665 van Veen, J.A. and Paul, E.A. (1979) Conversion of biovolume measurements of soil
666 organisms, grown under various moisture tensions, to biomass and nutrient
667 content. Appl. Environ. Microbiol. 37(4), 686-692.
668 Vanrolleghem, P., Van Daele, M. and Dochain, D. (1995) Practical identifiability of
669 biokinetic model of activated sludge respiration. Water Res. 29(11), 2561-2570.
670 Vavilin, V.A. and Angelidaki, I. (2005) Anaerobic degradation of solid material:
671 importance of initiation centers for methanogenesis, mixing intensity, and 2D
672 distributed model. Biotechnol. Bioeng. 89(1), 113-122.
673 Vavilin, V.A., Fernandez, B., Palatsi, J. and Flotats, X. (2008) Hydrolysis kinetics in
674 anaerobic degradation of particulate organic material: an overview. Waste
675 Manage. 28(6), 939-951.
676 Vavilin, V.A., Lokshina, L.Y., Jokela, J.P. and Rintala, J.A. (2004) Modeling solid
677 waste decomposition. Bioresour. Technol. 94(1), 69-81.
678 Vavilin, V.A., Rytov, S.V., Lokshina, L.Y., Pavlostathis, S.G. and Barlaz, M.A. (2003)
679 Distributed model of solid waste anaerobic digestion: effects of leachate
680 recirculation and pH adjustment. Biotechnol. Bioeng. 81(1), 66-73.
681 Xu, F., Li, Y. and Wang, Z.-W. (2015) Mathematical modeling of solid-state anaerobic
682 digestion. Prog. Energy Combust. Sci. 51, 49-66.
683
684
685 **Table 1**: Biochemical kinetics used for model implementation verification and
686 calibration.
687 **Table 2**: Influent and initial conditions used for model implementation verification and
688 model calibration.
689 **Table 3**: Summary of steady-state results for model implementation verification.
690 **Table 4**: Main parameters modified for model calibration.
691
692 **Figure 1**: High-solids vs. ‘wet’ anaerobic digestion.
693 **Figure 2**: Schematic representation of the high-solids anaerobic digestion model
694 implementation.
695 **Figure 3**: Hydraulic retention time and organic loading rate in model implementation
696 verification: a) ‘wet’ anaerobic digestion (simulations A and B); and b) high-solids
697 anaerobic digestion (simulations C and D).

698 **Figure 4**: Batch mono-digestion of OFMSW at 15 % total solids: a) accumulated
699 methane production and reactor mass content; b) volatile fatty acids; c) total and free
700 ammonia nitrogen; and d) total and volatile solids.
701
702

Table 1: Biochemical kinetics used for model implementation verification and calibration.

Process	Rate (ρ_j, kg COD m^{-3} d^{-1})	
	Model Verification	**Model Calibration**
Disintegration	$k_{dis}*X_c$	-
Hydrolysis of Carbohydrates	$k_{h,ch}*X_{ch}$	$k_{h,ch}*X_{ch}$
Hydrolysis of Proteins	$k_{h,pr}*X_{pr}$	$k_{h,pr}*X_{pr}$
Hydrolysis of Lipids	$k_{h,li}*X_{li}$	$k_{h,li}*X_{li}$
Sugars Uptake	$k_{m,su}*S_{su,App}/(K_{S,Xsu}+S_{su,App})*X_{su}*I_{pH}*I_{in}$	$k_{m,su}*S_{su,App}/(K_{S,Xsu}+S_{su,App})*X_{su}*I_{pH}*I_{in}$
Aminoacids Uptake	$k_{m,aa}*S_{aa,App}/(K_{S,Xaa}+S_{aa,App})*X_{aa}*I_{pH}*I_{in}$	$k_{m,aa}*S_{aa,App}/(K_{S,Xaa}+S_{aa,App})*X_{aa}*I_{pH}*I_{in}$
LCFA Uptake	$k_{m,fa}*S_{fa}/(K_{S,Xfa}+S_{fa})*X_{fa}*I_{pH}*I_{in}*I_{h2}$	$k_{m,fa}*S_{fa}/(K_{S,Xfa}+S_{fa})*X_{fa}*I_{pH}*I_{in}*I_{h2}$
Valerate Uptake	$k_{m,c4}*S_{va,App}/(K_{S,Xc4}+S_{va,App})*X_{c4}*S_{va,App}/(1+S_{bu,App}+10^{-6})*I_{pH}*I_{in}*I_{h2}$	$k_{m,c5}*S_{va,App}/(K_{S,Xc5}+S_{va,App})*X_{c5}*I_{pH}*I_{in}*I_{h2}$
Butyrate Uptake	$k_{m,c4}*S_{bu,App}/(K_{S,Xc4}+S_{bu,App})*X_{c4}*S_{bu,App}/(1+S_{bu,App}+10^{-6})*I_{pH}*I_{in}*I_{h2}$	$k_{m,c4}*S_{bu,App}/(K_{S,Xc4}+S_{bu,App})*X_{c4}*I_{pH}*I_{in}*I_{h2}$
Propionate Uptake	$k_{m,pro}*S_{pro,App}/(K_{S,Xpro}+S_{pro,App})*X_{pro}*I_{pH}*I_{in}*I_{h2}$	$k_{m,pro}*S_{pro,App}/(K_{S,Xpro}+S_{pro,App})*X_{pro}*I_{pH}*I_{in}*I_{h2}$
Acetate Uptake	$k_{m,ac}*S_{acApp}/(K_{S,Xac}+S_{ac,App})*X_{ac}*I_{pH}*I_{in}*I_{nh3}$	$k_{m,ac}*S_{ac,App}/(K_{S,Xac}+S_{ac,App})*X_{ac}*I_{pH}*I_{in}*I_{nh3}$
Hydrogen Uptake	$k_{m,h2}*S_{h2,App}/(K_{S,Xh2}+S_{h2,App})*X_{h2}*I_{pH}*I_{in}$	$k_{m,h2}*S_{h2,App}/(K_{S,Xh2}+S_{h2,App})*X_{h2}*I_{pH}*I_{in}$
Sugar Degraders Decay	k_d*X_{su}	k_d*X_{su}
Aminoacids Degraders Decay	k_d*X_{aa}	k_d*X_{aa}
LCFA Degraders Decay	k_d*X_{fa}	k_d*X_{fa}
Valerate Degraders Decay	-	k_d*X_{c5}
Butyrate Degraders Decay	k_d*X_{c4}	k_d*X_{c4}
Propionate Degraders Decay	k_d*X_{pro}	k_d*X_{pro}
Acetate Degraders Decay	k_d*X_{ac}	k_d*X_{ac}
Hydrogen Degraders Decay	k_d*X_{h2}	k_d*X_{h2}

with
$$I_{in} = S_{in,App}/(K_{S,Sin}+S_{in,App})$$
$$I_{h2} = K_{i,Sh2}/(K_{i,Sh2} + S_{h2,App})$$
$$I_{pH} = K_{pH}\text{^}N_{pH}/(K_{pH}\text{^}N_{pH} + S_{h+}\text{^}N_{pH})$$
$$I_{nh3} = K_{i,Snh3}/(K_{i,Snh3} + S_{nh3,App})$$

Table 2: Influent and initial conditions used for model implementation verification and model calibration.

Name	Model Verification			Model Calibration	Units
	Simulation A	Simulation B	Simulations C & D		
S_{su}	0.010	0.010	0.010	13.557	kg COD m^{-3}
S_{aa}	0.001	0.001	0.001	2.207	kg COD m^{-3}
S_{fa}	0.001	0.001	0.001	1.393	kg COD m^{-3}
S_{va}	0.001	0.001	0.001	0.734	kg COD m^{-3}
S_{bu}	0.001	0.001	0.001	0.500	kg COD m^{-3}
S_{pro}	0.001	0.001	0.001	2.059	kg COD m^{-3}
S_{ac}	0.001	0.001	0.001	0.103	kg COD m^{-3}
S_{h2}	1.000E-08	1.000E-08	1.000E-08	1.000E-08	kg COD m^{-3}
S_{ch4}	1.000E-08	1.000E-08	1.000E-08	1.000E-08	kg COD m^{-3}
S_{ic}	0.040	0.040	0.040	0.029	kmol C m^{-3}
S_{in}	0.010	0.010	0.010	0.186	kmol N m^{-3}
S_{i}	0.020	0.020	0.020	0.000	kg COD m^{-3}
$S_{i,subs}$	-	-	-	32.227	kgCOD m^{-3}
X_{c}	2.000	2.000	2.000	-	kg COD m^{-3}
X_{ch}	5.000	5.000	120.000	40.671	kg COD m^{-3}
X_{pr}	20.000	20.000	20.000	30.902	kg COD m^{-3}
X_{g}	5.000	5.000	5.000	12.534	kg COD m^{-3}
X_{su}	0.010	0.010	0.010	0.050	kg COD m^{-3}
X_{aa}	0.010	0.010	0.010	0.050	kg COD m^{-3}
X_{fa}	0.010	0.010	0.010	0.001	kg COD m^{-3}
X_{c5}	-	-	-	0.010	kgCOD m^{-3}
X_{c4}	0.010	0.010	0.010	0.002	kg COD m^{-3}
X_{pro}	0.010	0.010	0.010	0.005	kg COD m^{-3}
X_{ac}	0.010	0.010	0.010	0.003	kg COD m^{-3}
X_{h2}	0.010	0.010	0.010	0.070	kg COD m^{-3}
X_{i}	25.000	25.000	250.000	0.000	kg COD m^{-3}
$X_{i,subs}$	-	-	-	80.567	kgCOD m^{-3}
S_{cat}	0.040	0.040	0.040	0.100	kmoleq m^{-3}
S_{an}	0.020	0.020	0.020	0.051	kmoleq m^{-3}
ρ_{Global}	-	1000.000	1100.000	1077.633	kg m^{-3}
TS	-	4.500	25.000	15.502	%
VS	-	3.500	23.000	12.942	%

Table 3: Summary of steady-state results for model implementation verification.

Variable	ADM1 Implementation		HS-AD Model Implementation			Units
	Rosen & Jeppsson (2006)	'Wet' AD	'Wet' AD Const. Effluent**	HS-AD Const. Effluent**	HS-AD Variable Effluent	
S_{su}	0.01195	0.01195	0.01269	0.01692	0.01000	kg COD m^{-3}
S_{ac}	0.19763	0.19721	0.27484	0.16339	0.05707	kg COD m^{-3}
S_{ic}	0.15268	0.15270	0.15232	0.11377	0.11028	kmole C m^{-3}
S_{in}	0.13023	0.13023	0.13129	0.08451	0.07803	kmole N m^{-3}
X_{ch}	0.02795	0.02795	0.03183	60.73693	41.21685	kg COD m^{-3}
X_{su}	0.42017	0.42017	0.43628	5.38786	6.15898	kg COD m^{-3}
X_{ac}	0.76056	0.76058	0.78837	2.35994	2.52894	kg COD m^{-3}
$Q_{Effluent}$	170	170	170	170	160	m^3 d^{-1}
pH	7.47	7.46	7.48	7.20	7.16	m^3 d^{-1}
S_{co2}	0.0099	0.0099	0.0096	0.0128	0.0134	kmol C m^{-3}
S_{nh3}	0.0041	0.0041	0.0042	0.0015	0.0012	kmol N m^{-3}
P_T	1.069	1.069	1.069	1.180	1.220	bar
Q_g	2956	2956	2939	9752	12472	Nm^3 d^{-1}
$\%CH_4$	61*	60.9	60.8	50.6	49.9	%
$\%CO_2$	34*	33.9	34.0	44.7	45.5	%
V_{Global}	3400	3400	2967	1717	3400	m^3
$\rho_{Global0}$	-	1000	1000	1100	1100	kg m^{-3}
ρ_{Global}	-	1000	995	1082	1077	kg m^{-3}
HRT	20*	20	20	20	20	d
HRT_{real}	-	20	17	10	20	d
OLR	-	2.85	2.85	19.85	19.85	kg COD m^{-3} d^{-1}
OLR_{real}	-	2.85	3.27	39.32	19.86	kg COD m^{-3} d^{-1}
TS_0	4.5*	-	4.5	25.0	25.0	%
TS	-	-	2.9	20.4	19.0	%
TS_{Recalc}	-	-	1.9	19.8	18.5	%
VS_0	-	-	3.5	23.0	23.0	%
VS	-	-	1.8	18.2	16.9	%
VS_{Recalc}	-	-	0.9	17.6	16.3	%

**Mentioned Only; **No Steady-State Reached.*

Table 4: Main parameters modified for model calibration.

Parameter	ADM1	This Study	Units
$k_{h,ch}$	10	0.05	d^{-1}
$k_{h,pr}$	10	0.05	d^{-1}
$k_{h,li}$	10	0.07	d^{-1}
$k_{m,su}$	70	35	d^{-1}
$k_{m,fa}$	10	4	d^{-1}
$k_{m,c5}$	30	1	d^{-1}
$k_{m,c4}$	30	6	d^{-1}
$k_{m,pro}$	20	1	d^{-1}
$pH_{LL,ac}$	6	5.8	
$pH_{UL,ac}$	7	6.8	
$f_{bu,su}$	0.13	0.37	
$f_{pro,su}$	0.27	0.11	
$f_{ac,su}$	0.41	0.40	
$f_{h2,su}$	0.19	0.12	
$N_{i,subs}$	-	0.001	kmol N m^{-3}

'Wet' Anaerobic Digestion

$Q_0 = Q_e = Q$

V_{Global} = const.

$$V_{Global}\frac{d\rho}{dt} = Q(\rho_0 - \rho) - \sum r_i$$

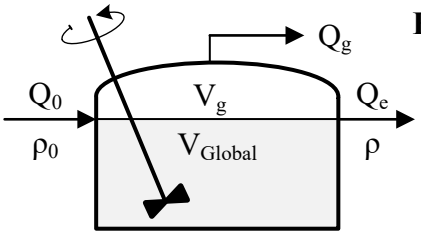

High-Solids Anaerobic Digestion

$Q_0 \neq Q_e$

$V_{Global} \neq$ const.

$$\frac{d(\rho V_{Global})}{dt} = \rho_0 Q_0 - \rho Q_e - \sum r_i$$

Figure 1: High-solids vs. 'wet' anaerobic digestion.

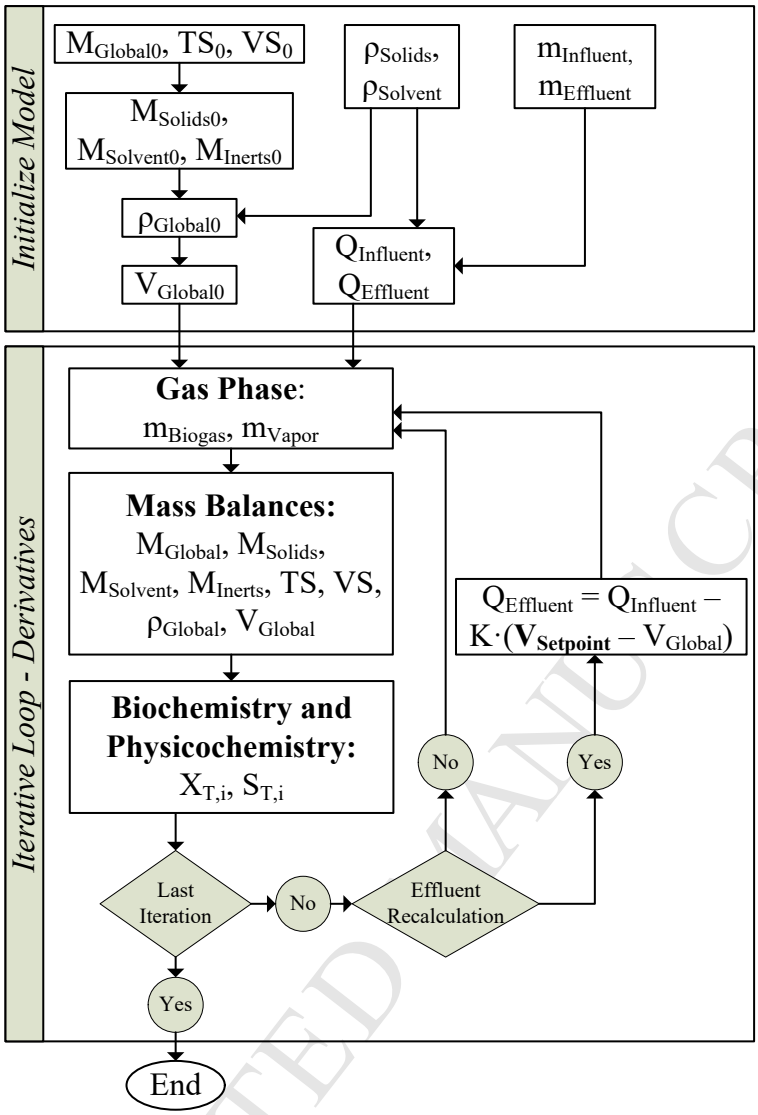

Figure 2: Schematic representation of the high-solids anaerobic digestion model implementation.

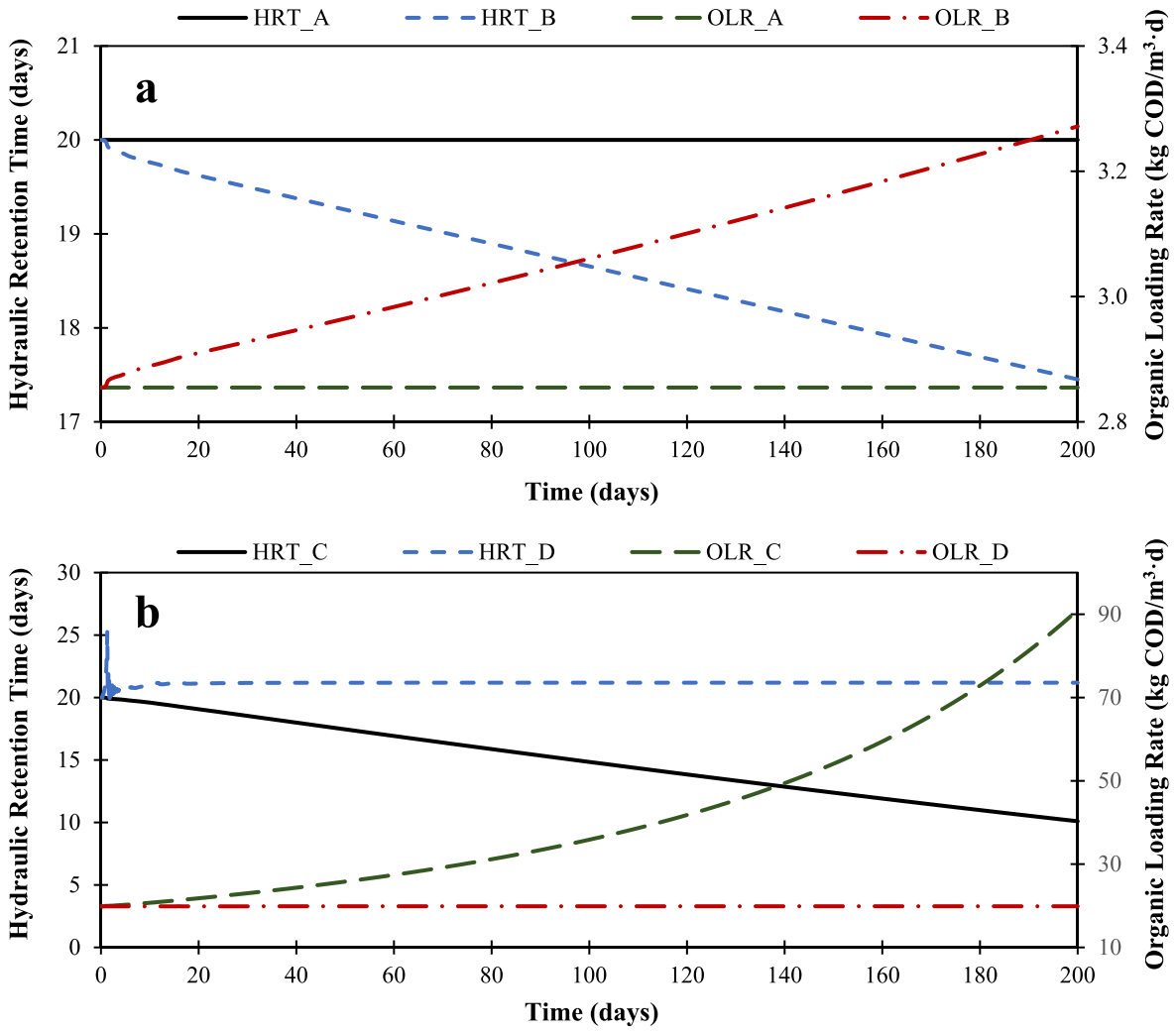

Figure 3: Hydraulic retention time and organic loading rate in model implementation verification: a) 'wet' anaerobic digestion (simulations A and B); and b) high-solids anaerobic digestion (simulations C and D).

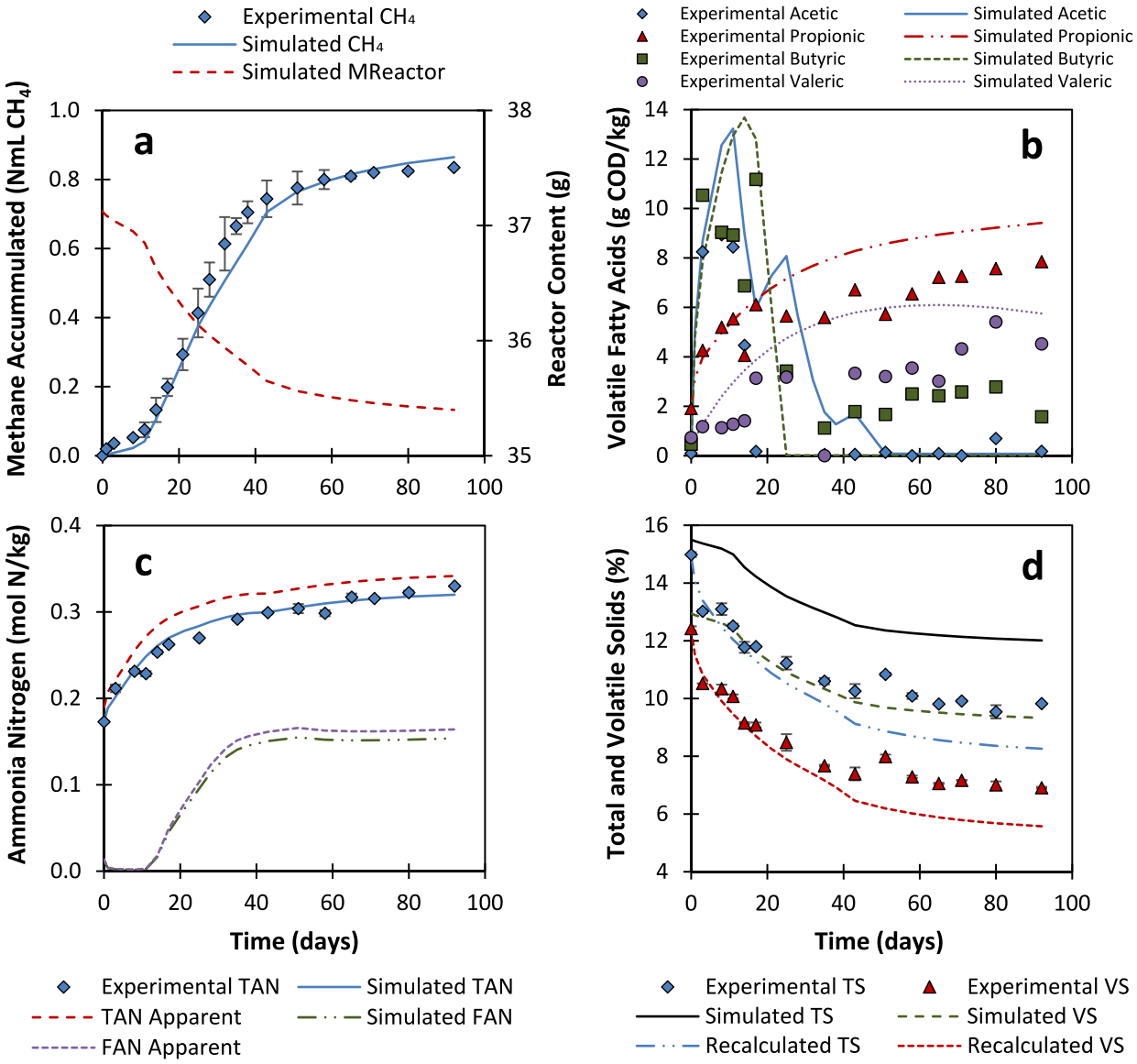

Figure 4: Batch mono-digestion of OFMSW at 15 % total solids: a) accumulated methane production and reactor mass content; b) volatile fatty acids; c) total and free ammonia nitrogen; and d) total and volatile solids.

Highlights

- A novel HS-AD model based on ADM1 was developed for homogenized reactors.
- Reactor mass/volume and total solids dynamics in HS-AD were simulated.
- The model considers the TS concentration effect on soluble species in HS-AD.
- The model simulated adequately VFA and TAN of HS-AD using OFMSW as substrate.